

Unitarity-limited elastic collision rate in a harmonically trapped Fermi gas

M. E. Gehm, S. L. Hemmer, K. M. O'Hara, and J. E. Thomas
Physics Department, Duke University, Durham, North Carolina 27708-0305, USA
 (Received 25 April 2003; published 23 July 2003)

We derive the elastic collision rate for a harmonically trapped Fermi gas in the extreme unitarity limit where the s -wave scattering cross section is $\sigma(k) = 4\pi/k^2$, with $\hbar k$ the relative momentum. The collision rate is given in the form $\Gamma = \gamma I(T/T_F)$ —the product of a universal collision rate $\gamma = k_B T_F / (6\pi\hbar)$ and a dimensionless function of the ratio of the temperature T to the Fermi temperature T_F . We find that I has a peak value of ≈ 4.6 at $T/T_F \approx 0.4$, $I \approx 82 (T/T_F)^2$ for $T/T_F \leq 0.15$, and $I \approx 2 (T_F/T)^2$ for $T/T_F > 1.5$. We estimate the collision rate for recent experiments on a strongly-interacting degenerate Fermi gas of atoms.

DOI: 10.1103/PhysRevA.68.011603

PACS number(s): 03.75.Ss, 32.80.Pj

I. INTRODUCTION

Recently, we [1] and several other groups [2–5] have begun exploring the strongly interacting regime in degenerate Fermi gases of atoms. In these experiments, a magnetic field is applied to the atomic samples to tune the interparticle interactions to the vicinity of a Feshbach resonance where the scattering length is large compared to the interparticle spacing. In this regime, new forms of high-temperature superfluidity are predicted [6–8] and strongly anisotropic expansion has been observed [1,4,5]. As we pointed out in Refs. [1,9], the strongly interacting regime leads to unitarity-limited mean-field interactions as well as unitarity-limited collision dynamics. In the latter case, the scattering cross section is of the order of $4\pi/k_F^2$, where k_F is the Fermi wave vector. In the unitarity limit, the collision rate assumes a universal form and is proportional to the Fermi energy $k_B T_F$. At sufficiently low temperatures, Pauli blocking may suppress the unitarity-limited elastic collision rate for the trapped gas, producing an effectively collisionless regime. However, a theoretical study of Pauli blocking in the unitarity-limited regime has not been presented previously, making it difficult to accurately estimate the collision rate. The primary purpose of this paper is to present such a treatment.

Several groups have examined the effects of Pauli blocking on the elastic collision rate for an energy-independent cross section [10–13]. For comparison to the collision rates obtained with a unitarity-limited cross section, we begin by deriving a formula for the collision rate in a harmonic trap as a function of temperature for an energy-independent cross section σ . The results reproduce those obtained in Ref. [12] within 10% [14]. We then extend the treatment to include the energy dependence of the cross section in the extreme unitarity limit, where the zero-energy scattering length a_S satisfies $|k_F a_S| \gg 1$ and the gas is strongly interacting. We show that the numerically calculated collision rates for both the energy-independent and unitarity-limited cross sections agree with analytic expressions derived for the high-temperature limit.

The final part of the paper defines a hydrodynamic parameter $\phi = \Gamma/\omega_\perp$, the ratio of unitarity-limited collision rate Γ to the transverse oscillation frequency ω_\perp of atoms in the trap. We calibrate ϕ by observing the threshold for hydrody-

namic expansion of a strongly interacting Fermi gas as a function of evaporation time [1]. We estimate ϕ for several recent experiments on strongly interacting Fermi gases [1,4,5].

II. CALCULATING THE COLLISION RATE

We consider a simple model that assumes that s -wave scattering is dominant [15]. In this case, the collision cross section takes the form

$$\sigma(k) = \frac{4\pi a_S^2}{1 + k^2 a_S^2}, \quad (1)$$

where k is the relative wave vector of a colliding pair of spin-up and spin-down fermionic atoms.

In the trap, the average collision rate per particle, Γ , is determined from the s -wave Boltzmann equation [16] under the assumption of sufficient ergodicity. We consider the rate for the process in which a spin-up and a spin-down atom of total energy $\epsilon_{\text{in}} = \epsilon_3 + \epsilon_4$ collide to produce atoms with total energy $\epsilon_{\text{out}} = \epsilon_1 + \epsilon_2$. The effects of Pauli blocking are included for the particles on the outgoing channel, and we assume a 50-50 mixture of atoms in the two spin states. The depletion term in the Boltzmann equation for the particle of energy ϵ_4 is integrated over ϵ_4 to determine the collision rate Γ for either spin state (as a collision inherently includes one atom of each spin). For an energy-independent cross section, the integrated loss rate is then $\dot{N}/2 \equiv -\Gamma N/2$, and

$$\begin{aligned} \Gamma \frac{N}{2} &= \frac{M\sigma}{\pi^2 \hbar^3} \int d\epsilon_1 d\epsilon_2 d\epsilon_3 d\epsilon_4 \mathcal{D}(\epsilon_{\text{min}}) \delta(\epsilon_1 + \epsilon_2 - \epsilon_3 - \epsilon_4) \\ &\times (1 - f_1)(1 - f_2)f_3 f_4, \end{aligned} \quad (2)$$

where Γ is the number of collisions per second per atom, N is the total number of atoms in the trap, and M is the atomic mass. Here, $\mathcal{D}(\epsilon_{\text{min}})$ is the density of states evaluated at the energy $\epsilon_{\text{min}} = \min\{\epsilon_1, \epsilon_2, \epsilon_3, \epsilon_4\}$. $f_i = 1/(g_i + 1)$ is the occupation number with $g_i = \exp[(\epsilon_i - \mu)/k_B T]$, and μ is the chemical potential [17]. At zero temperature, the chemical potential is given by the Fermi energy $\mu(0) = \epsilon_F = (3N)^{1/3} \hbar \bar{\omega}$

$=k_B T_F$, where $\bar{\omega} = (\omega_\perp^2 \omega_z)^{1/3}$ with ω_\perp and ω_z the transverse and axial trap oscillation frequencies of a cylindrically symmetric trap.

For fermions, the collision cross section of Eq. (1) with $|ka_S| \ll 1$ is $\sigma = 4\pi a_S^2$, i.e., half that for indistinguishable bosons. We begin by determining Γ for this case.

A. Energy-independent cross section

The integrand in Eq. (2) is readily shown to be symmetric under the interchange of all four particle labels. Hence, without loss of generality, we multiply the integrand by 4, and take $\epsilon_{\min} = \epsilon_1$ and $\mathcal{D}(\epsilon_{\min}) = [\epsilon_1^2 / (2\hbar^3 \bar{\omega}^3)] \theta_{21} \theta_{31} \theta_{41}$, where $\theta_{21} = \theta(\epsilon_2 - \epsilon_1)$ is a unit step function.

It is useful to write the collision rate as the product of a natural collision rate γ_{EI} , which depends on the trap parameters, and a dimensionless integral $I_{EI}(T/T_F)$, which describes the temperature dependence,

$$\Gamma = \gamma_{EI} I_{EI}(T/T_F). \quad (3)$$

We take the natural collision rate to be the classical collision rate at $T = T_F$,

$$\gamma_{EI} = \frac{NM \bar{\omega}^3 \sigma}{4\pi^2 k_B T_F}. \quad (4)$$

Note that the rate is 1/4 of that obtained in a spin-polarized Bose gas. With this choice, I_{EI} becomes

$$I_{EI}(T/T_F) = 144 \int \int \int_0^\infty dx_1 dx_2 dx_3 x_1^2 f(x_1 + x_2) f(x_1 + x_3) \times [1 - f(x_1)] [1 - f(x_1 + x_2 + x_3)]. \quad (5)$$

Here $f(x) = 1/[g(x) + 1]$, where $g(x) = \exp[(T_F/T)(x - \mu/\epsilon_F)]$. We assume that for the cases of interest, the trap depth is large compared to ϵ_F and $k_B T$.

I_{EI} is readily determined by numerical integration using standard results for the chemical potential as a function of T/T_F [17]. At low temperature, $T/T_F \leq 0.2$, we find that I_{EI} is well fit by $I_{EI}(T/T_F) \approx 15(T/T_F)^2$, which displays the quadratic dependence expected for Pauli blocking in both final states. At high temperature, $T/T_F > 1.5$, we find the expected temperature dependence, $I_{EI}(T/T_F) \approx T_F/T$, as shown below. The complete function $I_{EI}(T/T_F)$ is plotted in Fig. 1(a). The maximum value, $I_{EI} \approx 1.3$, occurs for $T/T_F \approx 0.5$. This demonstrates that γ_{EI} is essentially the maximum collision rate.

B. Unitarity-limited cross section

To include the energy dependence of the cross section, we adopt the notation of Ref. [16], and make the replacement

$$\sigma \mathcal{D}(\epsilon_{\min}) \rightarrow \frac{2\pi M}{(2\pi\hbar)^3} \int_{U(\mathbf{x}) < \epsilon_{\min}} d\mathbf{x} \int_{P_-(\mathbf{x})}^{P_+(\mathbf{x})} dP \sigma(q), \quad (6)$$

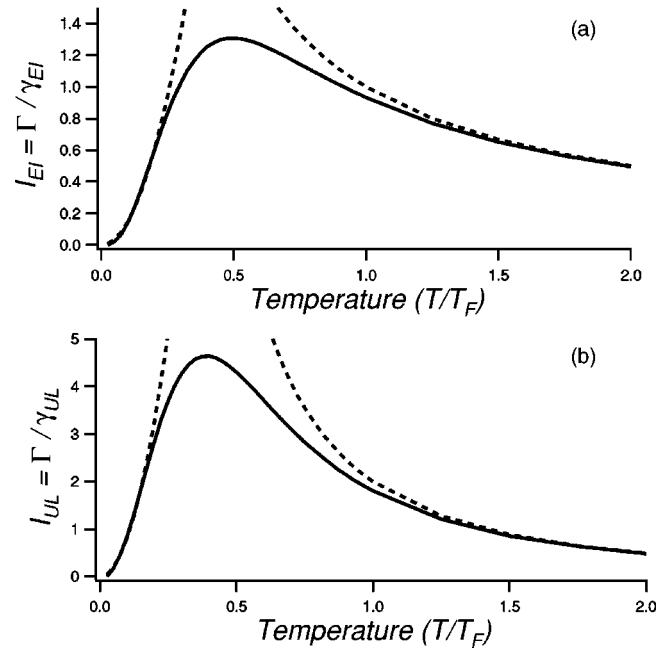


FIG. 1. Temperature dependence of the elastic-scattering collision rate Γ in units of the natural collision rate γ . The dashed lines indicate the high- and low-temperature approximations. (a) The collision rate for an energy-independent cross section. (b) The collision rate for a unitarity-limited cross section.

where $2q = \sqrt{P_+^2 + P_-^2 - P^2}$ determines the relative wave vector q , $P_\pm = \sqrt{2M[\epsilon - \epsilon_{\min} - U(\mathbf{x})] \pm \sqrt{2M[\epsilon_{\min} - U(\mathbf{x})]}}$, $U(\mathbf{x})$ is the trap potential, and ϵ is the total energy of the colliding particles.

We are interested in the extreme unitarity limit, where $\sigma(k) = 4\pi/k^2$ according to Eq. (1) and the elastic collision rate is the maximum possible [18]. We write the collision rate as

$$\Gamma = \gamma_{UL} I_{UL}(T/T_F). \quad (7)$$

The natural collision rate, Eq. 4 with $\sigma = 4\pi/k_F^2$ and $k_F^2 = 2Mk_B T_F/\hbar^2$, then takes the form

$$\gamma_{UL} = \frac{\epsilon_F}{6\pi\hbar}. \quad (8)$$

The dimensionless integral I_{UL} is similar to that of Eq. (5),

$$I_{UL}(T/T_F) = 144 \int_0^\infty dx_1 \int_0^\infty dx_2 \int_0^\infty dx_3 x_1^2 f(x_1 + x_2) \times f(x_1 + x_3) [1 - f(x_1)] [1 - f(x_1 + x_2 + x_3)] \times F(2x_1 + x_2 + x_3, x_1), \quad (9)$$

where $F(x, x_m)$ determines the energy-dependent cross section $\sigma(q) = 4\pi/q^2$ in units of $4\pi/k_F^2$. The arguments of $F(x, x_m)$ are $x = \epsilon/\epsilon_F$ and $x_m = \epsilon_{\min}/\epsilon_F$. As in Eq. (5), we take $x_m = x_1$ without loss of generality.

For a harmonic potential,

$$F(x, x_m) = \frac{16}{\pi\sqrt{2x_m}} \int_0^1 \frac{du u^2}{\sqrt{x-2x_m u^2}} \ln \left[\frac{\chi_+(\alpha, u)}{\chi_-(\alpha, u)} \right],$$

where $\chi_{\pm}(\alpha, u) = A(\alpha, u) \pm B(\alpha, u)$, $A(\alpha, u) = \alpha + 2(1 - 2u^2)$, $B(\alpha, u) = 2\sqrt{2(1-u^2)(\alpha-2u^2)}$, and $\alpha = x/x_m$.

We can simplify the form of the integrals in Eq. (9) by transforming from coordinates $\{x_1, x_2, x_3, u\}$ into coordinates $\{w, y, z, s\}$, where $w = x_1$, $y = (x_2 + x_3)/2x_1$, $z = (x_3 - x_2)/2x_1$, and $s = 1 - u^2$. After the transformation, we have

$$\begin{aligned} I_{\text{UL}}(T/T_F) &= 144 \int_0^{\infty} dy G(y) \int_0^{\infty} dw w^3 [1 - f(w)] \\ &\quad \times [1 - f(w(1+2y))] \\ &\quad \times \int_{-y}^y dz f[w(1+y+z)] f[w(1+y-z)] \end{aligned} \quad (10)$$

with $G(y)$ given by

$$G(y) = \frac{16}{\pi} \int_0^1 ds \sqrt{\frac{1-s}{s+y}} \{ \ln[s+y/2 + \sqrt{s(s+y)}] - \ln(y/2) \}. \quad (11)$$

Equation (10) is plotted in Fig. 1(b). The maximum collision rate is larger by a factor ≈ 4 than for an energy-independent cross section $\sigma = 4\pi/k_F^2$, consistent with estimates from radio-frequency measurements of the mean-field shift in Ref. [4]. For $T/T_F < 0.15$, we again find the quadratic temperature dependence that results from Pauli blocking, $I_{\text{UL}} \approx 82(T/T_F)^2$. In the high- T/T_F limit, we find $I_{\text{UL}} \approx 2(T_F/T)^2$. This matches the high-temperature prediction given below. The maximum value of $I_{\text{UL}} \approx 4.6$ occurs at $T/T_F \approx 0.4$.

C. Comparison with analytic high- T/T_F results

We check the numerical results for the temperature dependence of the rates by calculating the collision rate Γ_{HT} for $T \gg T_F$ directly from the phase-space s -wave Boltzmann equation [16] in the high- T/T_F limit, where the occupation number is given by a Boltzmann factor and Pauli blocking can be neglected. Including the dependence of the scattering cross section on the relative speed v_r , we find generally that

$$\Gamma_{\text{HT}} \frac{N}{2} = \int d\mathbf{x} n_{\uparrow}(\mathbf{x}) n_{\downarrow}(\mathbf{x}) \langle v_r \sigma(v_r) \rangle, \quad (12)$$

where the angled brackets denote an average over the relative velocity distribution for pairs of atoms and $\int d\mathbf{x} n_{\uparrow, \downarrow}(\mathbf{x}) = N/2$. Equation (12) has a simple physical interpretation: The spin-up atoms at position \mathbf{x} , i.e., $n_{\uparrow}(\mathbf{x}) d\mathbf{x}$, are hit by spin-down atoms at a rate $n_{\downarrow}(\mathbf{x}) \langle v_r \sigma(v_r) \rangle$. For an energy-independent cross section, we obtain $\Gamma_{\text{HT}} = \gamma_{\text{El}} T_F/T$ in agreement with the numerical results for $I_{\text{El}}(T/T_F)$ of Fig. 1(a). The temperature dependence in this limit arises from the flux, which is the product of the density and the relative velocity, i.e., $n \langle v_r \rangle \propto 1/T$. For the extreme unitarity-limited

cross section $\sigma = 4\pi/k^2$, with $Mv_r/2 = \hbar k$, we obtain $\Gamma_{\text{HT}} = \gamma_{\text{UL}} 2(T_F/T)^2$ in agreement with the numerical results for $I_{\text{UL}}(T/T_F)$ shown in Fig. 1(b). In this case, the $1/T^2$ temperature dependence arises because both the flux and the cross section vary as $1/T$.

III. HYDRODYNAMIC PARAMETER ϕ

The collisional state of a gas can be described by a hydrodynamic parameter ϕ which is the number of collisions that an atom experiences during a characteristic time scale. When ϕ is large, the gas is collisionally hydrodynamic, while when ϕ is small, the gas is collisionless. The actual values of ϕ which qualify as ‘‘large’’ or ‘‘small’’ are determined by calibration.

We choose the characteristic time scale to be $1/\omega$, and take $\phi = \Gamma/\omega$ where $\omega = \omega_{\perp}, \omega_z$ are the oscillation frequencies of atoms in the trap. These are also the natural time scales for ballistic expansion, where the size of the cloud scales as $\sqrt{1 + \omega^2 t^2}$ in each direction. In the unitarity-limited regime, and for a cylindrically symmetric trap with elongation parameter $\lambda = \omega_z/\omega_{\perp}$, we can write ϕ_{\perp} as

$$\phi_{\perp} = \frac{(3\lambda N)^{1/3}}{6\pi} I_{\text{UL}}(T/T_F) \quad (13)$$

with N the total number of atoms in the 50-50 mixture. Then, $\phi_z = \phi_{\perp}/\lambda$.

A. Calibrating ϕ

We now turn to the question of determining the approximate value of ϕ for which the transition between collisionless and collisional behaviors occurs. In Ref. [1], we investigated the anisotropic expansion properties of a strongly interacting, degenerate Fermi gas of ${}^6\text{Li}$. When released from a highly elongated trap, the originally narrow dimensions of the gas expanded rapidly, while the broad dimension remained largely unchanged—inverting the aspect ratio of the cloud after 1 ms of expansion. We have studied how the observed aspect ratio of the expanded cloud varies with the duration of evaporative cooling. The aspect ratios are measured for a fixed expansion time of 600 μs and are compared to the predictions of ballistic and hydrodynamic expansion. The results are plotted in Fig. 2.

From this figure, we see that the hottest clouds (short evaporation times) expand ballistically, while the coldest clouds (longest evaporation times) expand hydrodynamically. Ballistic expansion is expected in a normal, collisionless gas. Since the rapid transverse expansion extinguishes collisions before the axial distribution can change significantly, the collisional behavior of the expanding gas can be associated with ϕ_{\perp} . For the shortest evaporation times shown in Fig. 2, we observe ballistic scaling with $T = 3T_F$ and $N = 4 \times 10^5$. For our trap, the initial aspect ratio $\lambda = 0.035$. From Eq. (13), we obtain $\phi_{\perp} = 0.4$ which then corresponds to approximately collisionless behavior. Therefore, $\phi = 0.4$ is, in general, the condition for collisionless behavior for any time scale $1/\omega$.

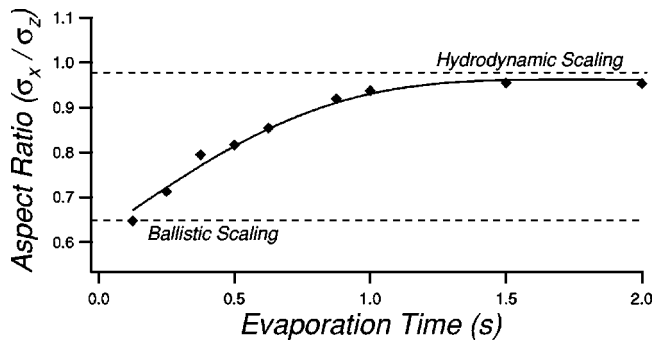


FIG. 2. Observed aspect ratio of a strongly interacting Fermi gas after $600 \mu\text{s}$ free expansion as a function of evaporation time. The aspect ratios corresponding to ballistic and hydrodynamic expansion are indicated by the dashed, horizontal lines, calculated as in Ref. [1]. The solid curve has been included to guide the eye. The gas evolves smoothly from ballistic expansion to hydrodynamic expansion as the evaporation time is increased.

B. Application to experiment

In addition to our work in Ref. [1], several groups have also recently observed hydrodynamic expansion of a Fermi gas in the strongly interacting regime [4,5]. The authors of these papers claim that their experiments are collisionally hydrodynamic. For Ref. [4], we take the total number of atoms $N=2.4 \times 10^5$ and $T/T_F=0.34$, with $\lambda=0.016$, yielding $I_{UL}=4.5$ and $\phi_{\perp}=5.4$. For Ref. [5], we take $N=7 \times 10^4$, $T/T_F=0.6$, and $\lambda=0.35$, yielding $I_{UL}=3.5$ and $\phi_{\perp}=7.7$. Hence, we agree with their conclusions.

Our experiments [1] produce strongly interacting Fermi gases at considerably lower temperatures. In those experiments, the total number of atoms is $N \approx 1.5 \times 10^5$ for tem-

peratures $0.08 \leq T/T_F \leq 0.2$. Equation 13 yields $0.7 \leq \phi_{\perp} \leq 3.7$, while $20 \leq \phi_z \leq 106$. The values of ϕ corresponding to our lowest temperatures indicate that the trapped gas is nearly collisionless on the transverse time scale, but collisional on the axial.

The onset of high-temperature superfluidity has been recently predicted in the temperature range $T/T_F=0.25-0.5$ [6–8]. Since Pauli blocking is ineffective for the unitarity-limited cross section when $T/T_F \geq 0.25$, it is not clear how collisions in the normal component will affect the formation of this high-temperature superfluid.

For an expanding gas, we cannot make a definitive statement about its collisional nature, even if it were collisionless when trapped, as Pauli blocking may become ineffective as a result of nonadiabaticity in the expansion, deformation of the Fermi surface, or through other effects [19]. The magnitude of these effects, and to what extent they modify ϕ , remains an open question. We are, therefore, working on experiments which will directly determine if the gas contains a superfluid fraction.

ACKNOWLEDGMENTS

We are indebted to J. T. M. Walraven for stimulating correspondence regarding this work. This research was supported by the Physics Divisions of the Army Research Office and the National Science Foundation, the Fundamental Physics in Microgravity Research program of the National Aeronautics and Space Administration, and the Chemical Sciences, Geosciences and Biosciences Division of the Office of Basic Energy Sciences, Office of Science, U.S. Department of Energy.

[1] K.M. O'Hara *et al.*, *Science* **298**, 2179 (2002).
 [2] K. Dieckmann *et al.*, *Phys. Rev. Lett.* **89**, 203201 (2002).
 [3] S. Jochim *et al.*, *Phys. Rev. Lett.* **89**, 273202 (2002).
 [4] C. Regal and D.S. Jin, *Phys. Rev. Lett.* **90**, 230404 (2003).
 [5] T. Bourdel *et al.*, e-print cond-mat/0303079.
 [6] M. Holland *et al.*, *Phys. Rev. Lett.* **87**, 120406 (2001).
 [7] E. Timmermans *et al.*, *Phys. Lett. A* **285**, 228 (2001).
 [8] Y. Ohashi and A. Griffin, *Phys. Rev. Lett.* **89**, 130402 (2002).
 [9] M.E. Gehm *et al.*, *Phys. Rev. A* **68**, 011401(R) (2003).
 [10] G. Ferrari, *Phys. Rev. A* **59**, R4125 (1999).
 [11] W. Geist *et al.*, *Phys. Rev. A* **61**, 013406 (2000); W. Geist and T.A.B. Kennedy, *ibid.* **65**, 063617 (2002).
 [12] M.J. Holland, B. DeMarco, and D.S. Jin, *Phys. Rev. A* **61**, 053610 (2000).
 [13] B. DeMarco, S.B. Papp, and D.S. Jin, *Phys. Rev. Lett.* **86**,

5409 (2001).

[14] We take into account a factor of 2 difference between our definition of the collision rate and that of Ref. [12]. We assume the thermal energy to be much smaller than the trap depth while Ref. [12] assumes a truncated distribution to treat evaporation.
 [15] We neglect higher-order partial-wave resonances. These sometimes occur near an *s*-wave scattering resonance. Carl Williams (private communication).
 [16] O.J. Luiten *et al.*, *Phys. Rev. A* **53**, 381 (1996).
 [17] D.A. Butts and D.S. Rokhsar, *Phys. Rev. A* **55**, 4346 (1997).
 [18] In the unitarity limit, the mean field rescales the trap radii and maintains a Thomas-Fermi density profile [9].
 [19] Henning Heiselberg, Jason Ho, and Wolfgang Ketterle (private communication).